AMERICAN SOCIETY FOR MICROBIOLOGY | Journal of Bacteriology®

RESEARCH ARTICLE

An *ompR-envZ* Two-Component System Ortholog Regulates Phase Variation, Osmotic Tolerance, Motility, and Virulence in *Acinetobacter baumannii* Strain AB5075

Kyle A. Tipton,[a] Philip N. Rather[a,b]

Department of Microbiology and Immunology, Emory University School of Medicine, Atlanta, Georgia, USA[a]; Research Service, Atlanta VA Medical Center, Decatur, Georgia, USA[b]

ABSTRACT Recently, a novel phase-variable colony opacity phenotype was discovered in *Acinetobacter baumannii* strain AB5075, where colonies interconvert between opaque and translucent variants. Opaque colonies become mottled or sectored after 24 h of growth due to translucent variants arising within the colony. This easily distinguishable opaque-colony phenotype was used to screen for random transposon insertions that increased the frequency of sectoring at a time point when wild-type colonies were uniformly opaque. A colony was identified that contained multiple papillae of translucent variants, and the insertion in this mutant mapped to an ortholog of the two-component system response regulator *ompR*. Subsequent investigation of in-frame deletions of *ompR* and the sensor kinase *envZ* (located adjacent to *ompR*) showed that the switching frequency from opaque to translucent was increased 401- and 281-fold, respectively. The *ompR* mutant also exhibited sensitivity to sodium chloride in growth medium, whereas the *envZ* mutation did not elicit sensitivity to sodium chloride. Mutation of either gene reduced motility in *A. baumannii* strain AB5075, but a mutation in both *ompR* and *envZ* produced a more profound effect. The *ompR* and *envZ* genes were cotranscribed but were not subject to autoregulation by OmpR. Both *ompR* and *envZ* mutant opaque variants were attenuated in virulence in the *Galleria mellonella* infection model, whereas mutation of *ompR* had no effect on the virulence of the translucent variant.

IMPORTANCE *Acinetobacter baumannii* is a well-known antibiotic-resistant pathogen; many clinical isolates can only be treated by a very small number of antibiotics (including colistin), while some exhibit panresistance. The current antimicrobial arsenal is nearing futility in the treatment of *Acinetobacter* infections, and new avenues of treatment are profoundly needed. Since phase variation controls the transition between opaque (virulent) and translucent (avirulent) states in *A. baumannii*, this may represent an "Achilles' heel" that can be targeted via the development of small molecules that lock cells in the translucent state and allow the host immune system to clear the infection. A better understanding of how phase variation is regulated may allow for the development of methods to target this process. The *ompR-envZ* two-component system ortholog negatively regulates phase variation in *A. baumannii*, and perturbation of this system leads to the attenuation of virulence in an invertebrate infection model.

KEYWORDS *Acinetobacter*, phase variation, osmotic stress

Received 28 September 2016 **Accepted** 14 November 2016

Accepted manuscript posted online 21 November 2016

Citation Tipton KA, Rather PN. 2017. An *ompR-envZ* two-component system ortholog regulates phase variation, osmotic tolerance, motility, and virulence in *Acinetobacter baumannii* strain AB5075. J Bacteriol 199:e00705-16. https://doi.org/10.1128/JB.00705-16.

Editor Piet A. J. de Boer, Case Western Reserve University School of Medicine

Address correspondence to Philip N. Rather, prather@emory.edu.

The Gram-negative bacterium *Acinetobacter baumannii* is well recognized as an opportunistic pathogen, part of a group of nosocomial pathogens (ESKAPE organisms), which merit increased investigation due to their presence in the nosocomial

environment and the development of broad-spectrum and panresistant isolates (1, 2). *A. baumannii* is also known as a pathogen of combat wound injuries in soldiers serving in dry desert climates (3). In the nosocomial environment and in intensive care units specifically, *A. baumannii* has taken up residence and has become challenging to treat due to its ability to acquire antibiotic resistance determinants (4–6). Clinicians treating *A. baumannii* infections today have few treatment options; the carbapenems and colistin are "last line of defense" drugs that are losing efficacy, indicating that novel approaches to fighting infections are profoundly needed (7–9).

Considering the relative wealth of knowledge concerning antibiotic resistance in *A. baumannii*, there are many unanswered questions regarding the organism's physiology and pathogenesis. Recently, a novel phase-variable mechanism was characterized that allows *A. baumannii* to interconvert between two phases or variants (opaque and translucent) that display markedly different phenotypes (10). Opaque variants (O) are more virulent and more motile and produce more 3-hydroxy-dodecanoyl-L-homoserine lactone (3-OH-C_{12}-HSL) autoinducer, whereas the translucent variants (T) form more robust biofilms, are less virulent, and are less motile. When cells are at high density, the colony variants interconvert at high frequency ($1/10^1$ to $1/10^2$), indicating that an epigenetic mechanism is likely governing phase variation in *A. baumannii*. Also, omission of sodium chloride from growth medium had a negative effect on switching for both variants (O to T; T to O) (10).

Two-component regulatory systems (TCS) in bacteria sense stimuli and respond to them by altering gene expression at the transcriptional level (11, 12). In the enteric pathogen *Escherichia coli*, the TCS OmpR/EnvZ governs outer membrane porin (OMP) expression in response to an osmotic signal (13). OmpR is a transcription factor and the cognate response regulator for the membrane-bound sensor kinase EnvZ (14–16). Aside from the regulation of outer membrane proteins (OMPs) in response to osmotic signals, OmpR and EnvZ act as global regulators controlling the expression of many genes (17). Uropathogenic *E. coli* persistence in the mouse urinary tract infection model and growth in human urine is also dependent on OmpR (18). Homologs of the OmpR/EnvZ TCS also control virulence in several other pathogens, including *Salmonella enterica* serovar Typhimurium, *Shigella flexneri*, and *Yersinia pestis* (19–21).

Through random transposon mutagenesis of *A. baumannii* strain AB5075, an insertion was located in the ABUW_0257 open reading frame (ORF) that shares significant homology (70% identity and 84% similarity at the amino acid level) to the OmpR transcriptional regulator from *E. coli*. This mutation was identified because it produced a very profound effect on colony morphology. The transposon insertion in the putative *ompR* ortholog led to decreased colony size for the opaque variant and activated phase switching in the opaque variant to interconvert at an extremely high frequency. This hyperswitching was made visible by the presence of translucent variants arising as papillae within opaque colonies. An in-frame deletion mutant in the putative *ompR* ORF was generated, and this mutant phenocopied the insertional mutant. Investigation of the *ompR* deletion mutant indicated that phase variation frequency from the opaque to translucent variant increased dramatically, sensitivity to osmotic pressure in growth medium increased, and motility decreased. Mutation of the sensor kinase *envZ* also activated phase variation from the opaque to translucent variant and decreased motility slightly, but this mutation had no effect on sensitivity to osmotic stress. In addition, OmpR and EnvZ in *A. baumannii* strain AB5075 are required for virulence of the O variant in the *Galleria mellonella* infection model.

RESULTS

The *A. baumannii* OmpR/EnvZ orthologs control opaque variant colony morphology and phase variation switching frequency. Opaque variant colonies develop a sectored or mottled appearance when grown for 24 h or more at 37°C, which denotes phase switching from the opaque to the translucent variant (10). This visual indication was utilized as a marker to screen for transposon insertions that would increase sectoring after 24 h of incubation. A small library of approximately 1,000 random

mutants were investigated, and one mutant, AB-Tn-6A, produced opaque colonies which had irregular edges and were speckled with papillae that resembled translucent variants. The transposon was found to have inserted 169 bp downstream from the start codon of ABUW_0257, which encodes an OmpR ortholog (70% identity and 84% similarity at the amino acid level). A Δ*ompR* in-frame deletion mutant (KT4) was constructed, and opaque colonies of this mutant exhibited altered colony morphology (similar to AB-Tn-6A) compared to the wild-type strain AB5075 opaque and translucent variants (Fig. 1A to C). The Δ*ompR* mutant opaque variant switching frequency was determined from colonies grown for 24 h, and the switching frequency significantly increased by 401-fold ($P < 0.0001$) compared to the wild-type strain AB5075 opaque variant (Fig. 1D). Deletion of the putative *envZ* gene or of both genes of the TCS yielded similar results with altered opaque colony morphology and vastly elevated switching frequency from opaque to translucent variant (281- and 463-fold increases, respectively [$P < 0.0001$ for both]) (Fig. 1D). This indicates that the *ompR-envZ* TCS is repressing phase variation and suggests that the phase variation process can be influenced by sensing of environmental factors in *A. baumannii* strain AB5075.

Interestingly, the Δ*ompR*, Δ*envZ* (strain KT5), or Δ*ompR* Δ*envZ* (strain KT6) mutations had no effect on translucent variant colony appearance (i.e., the size and shape of the colonies [data not shown]). This suggests that two unrelated mechanisms or processes govern the O-to-T versus the T-to-O switch. In addition, the switching frequency from T to O was low compared to the O-to-T switch, and only the Δ*envZ* mutant exhibited increased switching frequency (5-fold [$P < 0.0001$]). The Δ*ompR* mutant switching frequency from translucent to opaque was repressed (9-fold [$P = 0.5226$]), and the deletion of both genes had no effect on T-to-O switching (Fig. 1E).

Complementation analysis of the *ompR* operon mutants. To ensure that the increase in switching frequency that occurs in the opaque variant containing the Δ*ompR*, Δ*envZ*, and Δ*ompR* Δ*envZ* mutations was due to each mutation, complementation analysis was conducted by cloning the chromosomal version of each gene with its native ribosome binding site (RBS) into pWH1266 such that transcription is driven by the *bla* promoter (22). Phase switching in each mutant was restored to the wild-type level by providing intact alleles of each gene when expressed from a non-native promoter (Table 1). The phase variation frequency was reduced by 466-, 446-, and 1,152-fold in the Δ*ompR* ($P < 0.0001$), Δ*envZ* ($P = 0.4188$), and Δ*ompR* Δ*envZ* ($P = 0.0001$) mutants with complementation, respectively. This indicates that the effects on phase variation are produced by the deletions and not second-site mutations.

OmpR controls the response to osmotic stress. OmpR is known to play a role in the osmotic stress response in *E. coli*, growth of the Δ*ompR* mutant in broth culture was investigated (13). Figure 2A shows that the Δ*ompR* and the Δ*ompR* Δ*envZ* mutants exhibit an extended lag phase when grown in Luria-Bertani (LB) medium that can be abolished by removing sodium chloride from the growth medium. This suggests that OmpR regulation is homologous to what is seen in *E. coli* with regard to osmotic stress adaptation (18). The translucent variants of the Δ*ompR* and Δ*ompR* Δ*envZ* mutants also exhibited sensitivity to osmotic stress similar to that of the opaque variants, indicating that this effect is based on the mutation and not on the phase of the variant being investigated (see Fig. S1A in the supplemental material). However, the Δ*envZ* mutation did not exhibit the same sensitivity to sodium chloride (Fig. 2A). Supplying *ompR* in *trans* in the Δ*ompR* mutant nullified the growth defect observed in LB medium with sodium chloride (Fig. 2B). Titration of sodium chloride into the growth medium increased the lag phase in the Δ*ompR* mutant, and this effect is similar in the opaque and translucent variants (Fig. 2C and see Fig. S1B in the supplemental material). Sodium chloride concentration did not affect growth of the wild-type strain AB5075 opaque or translucent variant (data not shown). Supplementation of growth medium with sucrose also had a negative effect on growth of the Δ*ompR* mutant, which indicates that this effect is due to osmotic stress and is not specific for sodium chloride (see Fig. S2 in the supplemental material). These data indicate that the OmpR/EnvZ TCS in *A. baumannii*

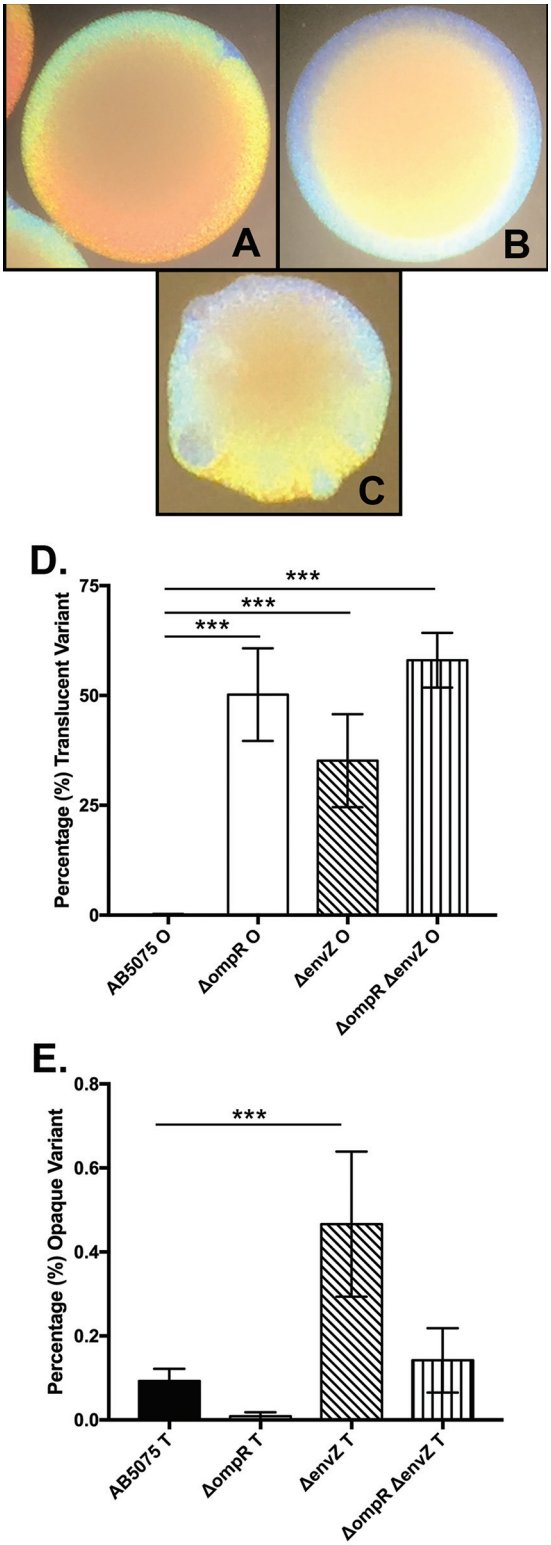

FIG 1 OmpR controls colony morphology and phase variation. *A. baumannii* colonies were photographed through a dissecting scope with oblique illumination from below after 24 h of growth. (A) Wild-type strain AB5075 opaque variant; (B) wild-type strain AB5075 translucent variant; (C) KT4 (Δ*ompR*) mutant. (D) Phase variation frequency represented as percentages of translucent variants in 24-h-old colonies of *A. baumannii* opaque colonies. Data are presented as the averages ± the standard deviations for six separate colonies. (E) Phase variation frequency represented as percentages of opaque variants in 24-h-old colonies of *A. baumannii* translucent colonies. Data are presented as the averages ± the standard deviations for six separate colonies. ***, $P < 0.0001$.

TABLE 1 Complementation of elevated phase variation in 24-h-old colonies

A. baumannii strain	Plasmid	Phase variation frequency (%) ± SD	Fold change	*P* value
AB5075 (wild type)	pWH1266	0.033 ± 0.022		
Δ*ompR* mutant (O variant)	pWH1266	61.6 ± 5.8		
	pompR	0.132 ± 0.189	466	<0.0001
Δ*envZ* mutant (O variant)	pWH1266	13.4 ± 10.6		
	penvZ	0.030 ± 0.027	446	0.4188
Δ*ompR* Δ*envZ* mutant (O variant)	pWH1266	43.8 ± 17		
	pompRenvZ	0.038 ± 0.017	1,152	0.0001

facilitates adaptation to alterations in environmental osmolarity in addition to a role in suppressing phase variation (Fig. 1 and Table 1).

The OmpR/EnvZ TCS is required for motility. In *E. coli*, OmpR is known to regulate expression of flagellar biosynthesis and motility (23). Although *A. baumannii* does not encode flagella, motility in this organism has been characterized (24–28). Furthermore, the opaque and translucent variants of *A. baumannii* strain AB5075 exhibit significant differences with regard to surface motility on soft agar plates (10). Since mutation of *ompR* and/or *envZ* yields increased phase variation from the opaque to translucent variant, motility by these mutants was assessed. Mutation of *ompR* reduced motility significantly (2.8-fold; $P < 0.0001$) in the opaque variant compared to the wild-type strain O variant, and this effect was increased when *ompR* and *envZ* were deleted together (4.3-fold; $P < 0.0001$) (Fig. 3A). The Δ*envZ* mutant was also less motile than the wild-type strain, but the difference was smaller than for the other mutants (1.4-fold; $P < 0.05$). While motility is lower overall in the T variant of each strain, a similar reduction in motility is evident when *ompR* ($p < 0.0001$), *envZ* ($P < 0.005$), or both genes ($P < 0.0001$) are mutated (Fig. 3B). Although the differences in motility displayed by the mutant T variants are statistically significant, the biological relevance of these effects are yet to be determined. Since the Δ*ompR* and Δ*ompR* Δ*envZ* mutants displayed sensitivity to sodium chloride, motility assays were performed without sodium chloride in the media to ensure that growth was not negatively affected. The Δ*envZ* mutant does not exhibit sensitivity to sodium chloride, which allowed for investigation of motility of the opaque variant of this mutant compared to the wild-type strain AB5075 opaque variant with or without sodium chloride. An inhibitory effect on motility of the wild-type strain AB5075 is apparent when sodium chloride is included in the agar (1.4-fold reduction, $P < 0.05$), but this effect is not present when *envZ* is mutated (see Fig. S3 in the supplemental material). Also, the inclusion of sodium chloride in motility assays shows that there is no significant difference between the wild-type strain AB5075 and the Δ*envZ* mutant ($P = 0.8324$). This result suggests that sodium chloride can repress motility in *A. baumannii* strain AB5075 in an EnvZ-dependent manner.

Biofilm formation is not affected by mutation of *ompR* or *envZ*. Biofilm formation in *E. coli* is known to be regulated by many factors, including OmpR (29, 30). The translucent variant of *A. baumannii* strain AB5075 produces more robust biofilms than the opaque variant on glass and polystyrene surfaces (10). Biofilm formation by the Δ*ompR*, Δ*envZ*, and Δ*ompR* Δ*envZ* mutant opaque and translucent variants was assessed, and no change in biofilm formation on polystyrene was apparent for any mutation in either the opaque or the translucent variant (see Fig. S4 in the supplemental material). These results suggest that OmpR/EnvZ do not regulate biofilm formation in *A. baumannii* strain AB5075 under the conditions tested.

The *ompR* gene is transcribed with *envZ* but is not regulated by OmpR. The *envZ* ORF (ABUW_0256) begins 18 bp downstream from the stop codon of *ompR*, and this suggests that the two genes are transcribed together as a polycistronic operon (Fig. 4A). The *ompR-envZ* operon structure was examined by synthesizing cDNA from wild-type strain AB5075 RNA with a primer specific to *envZ*. This cDNA was then used as the template for a PCR with primers to amplify a fragment of DNA spanning the

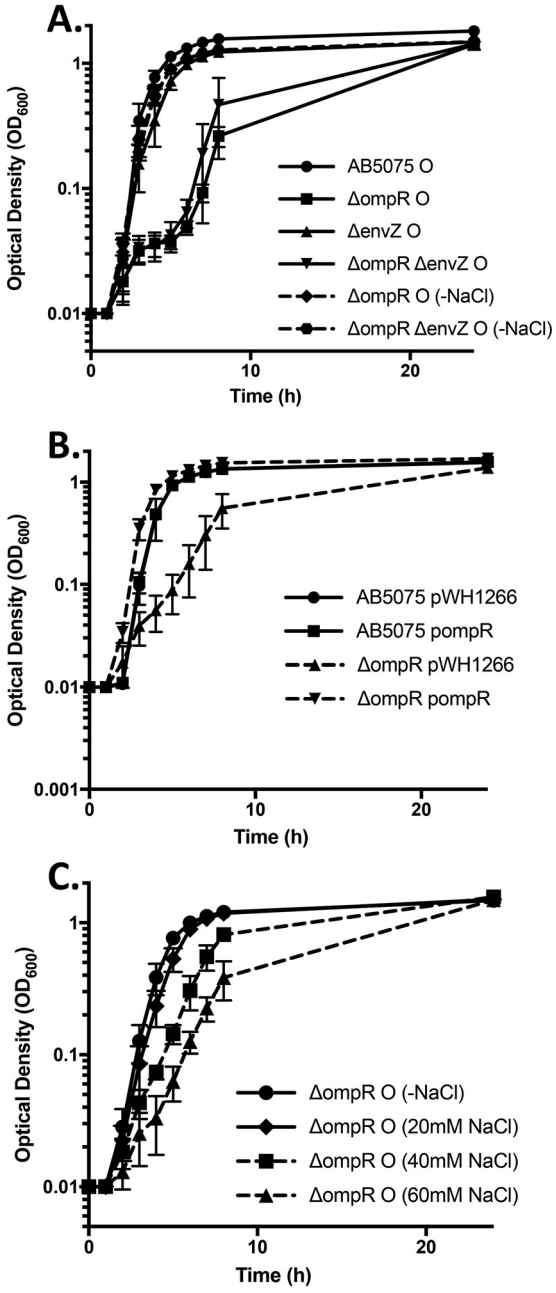

FIG 2 Deletion of *ompR* renders *A. baumannii* sensitive to osmolarity. The growth of *A. baumannii* was quantified over time by measuring the OD_{600}. (A) Growth curves in LB medium and in LB medium without sodium chloride over a 24-h period. Data are presented as the averages ± the standard deviations for three replicates. (B) Growth curves in LB medium over a 24-h period. Data are presented as the averages ± the standard deviations for three replicates. (C) Growth curves in LB medium with increasing concentrations of sodium chloride. Data are presented as the averages ± the standard deviations for three replicates.

intergenic region between *ompR* and *envZ*. Figure 4B shows that primers spanning the *ompR* intergenic region can be amplified from the *envZ*-specific cDNA. This suggests that *ompR* and *envZ* are transcribed together in an operon.

OmpR is known to act as a DNA-binding transcription factor, and regulation of the *ompR-envZ* transcript in the Δ*ompR* mutant was explored. Since a small segment of the *ompR* coding sequence is still present in the deletion mutant, quantitative real-time PCR (qRT-PCR) was utilized to examine expression of *ompR* in the Δ*ompR* mutant compared to the wild-type strain AB5075. The expression of *ompR* is only slightly

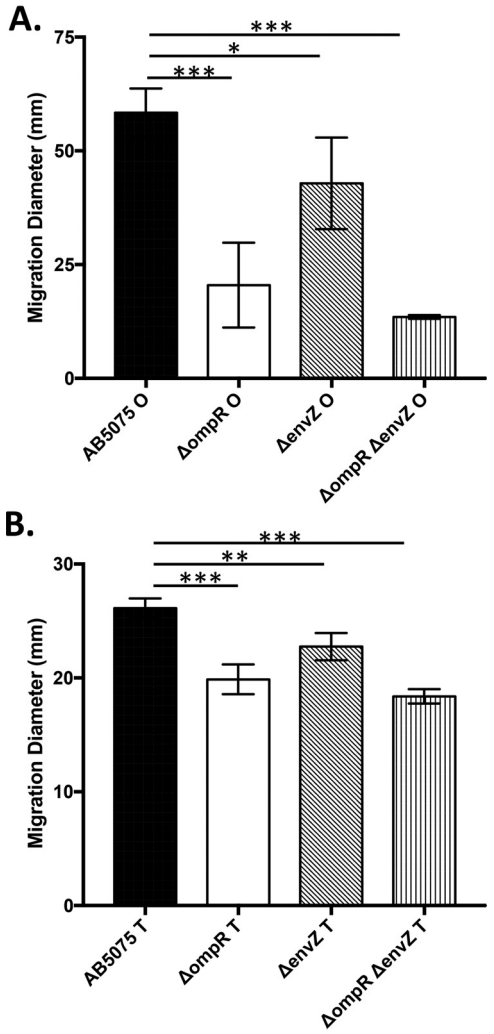

FIG 3 Motility in *A. baumannii* is controlled by OmpR/EnvZ. Cultures were grown in LB medium (−NaCl) to an OD_{600} of 0.3, and a 1-μl drop was then applied to the surface of 0.3% Eiken agar (−NaCl) plates, after which the plates were incubated at 37°C for ~9 h. Bars represent the average diameters of migration, with error bars representing the standard deviations. (A) Motility quantifications for opaque variants of the wild-type strain AB5075, the Δ*ompR* mutant (KT4), the Δ*envZ* mutant (KT5), and the Δ*ompR* Δ*envZ* double mutant (KT6). (B) Motility quantifications for translucent variants of the wild-type strain AB5075, the Δ*ompR* mutant (KT4), the Δ*envZ* mutant (KT5), and the Δ*ompR* Δ*envZ* double mutant (KT6). ***, $P < 0.0001$; **, $P < 0.005$; *, $P < 0.05$.

downregulated (1.51-fold; $P = 0.263$) in the Δ*ompR* mutant compared to the wild-type strain AB5075 (Fig. 4C). Also, the expression of the *envZ* gene was slightly downregulated (1.29-fold; $P = 0.5509$) in the Δ*ompR* mutant (Fig. 4C), suggesting that the *ompR* and *envZ* genes are not subject to autoregulation at the transcriptional level. Investigation of *ompR* and *envZ* expression in the wild-type strain AB5075 in the presence or absence of sodium chloride also showed that there is no difference in transcription of *ompR* or *envZ* under the conditions tested (Fig. 4D). These data support the finding that the genes are cotranscribed in a polycistronic operon, are not subject to autoregulation by OmpR, and do not respond to the salt concentrations tested here. However, these results do not rule out the possibility that *envZ* transcription could be driven by an undiscovered promoter that was not active under the conditions we tested.

OmpR does not regulate a putative OmpC ortholog or the outer membrane carboxylate channel (Occ) proteins. The outer membrane porins OmpF and OmpC are known to be regulated by OmpR in *E. coli* and allow for responding to changing

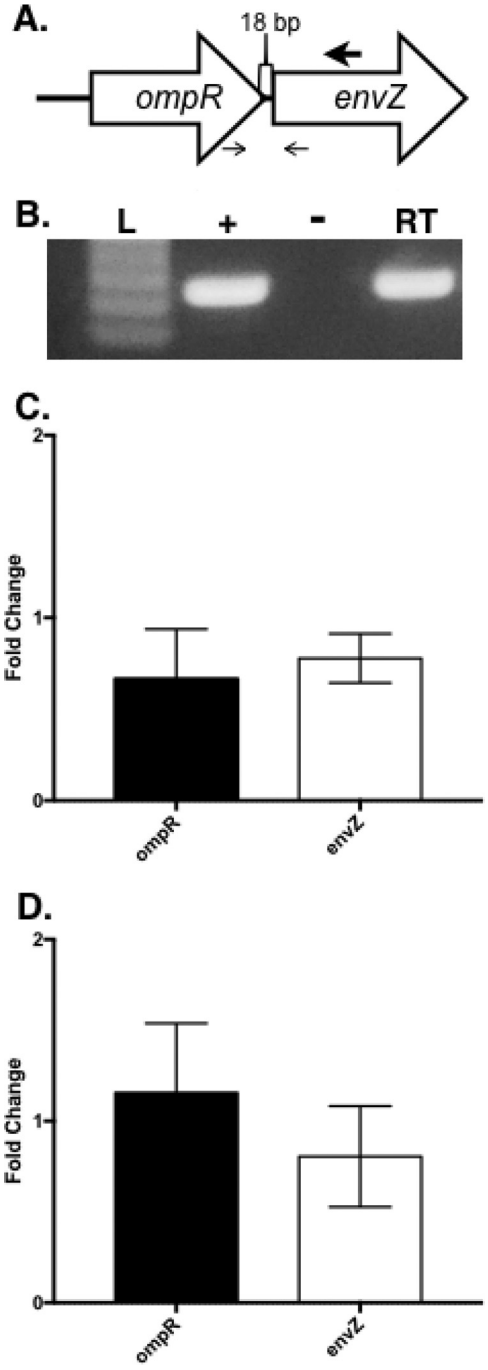

FIG 4 The *ompR-envZ* operon is not autoregulated. (A) Graphic depiction of the organization of the *ompR* locus from *A. baumannii* strain AB5075. The large arrow above the *envZ* gene denotes the location of the primer utilized in the reverse transcriptase reaction to produce *envZ*-specific cDNA. The small arrows below *ompR* and *envZ* denote the locations of the primers spanning the 18-bp intergenic region between *ompR* and *envZ*. (B) Gel picture of PCR product from transcript-specific cDNA (generated from wild-type AB5075 RNA) used as the template with primers that span the intergenic region between *ompR* and *envZ*. Reactions are labeled "+" for positive control with genomic DNA, "−" for negative control RNA without reverse transcriptase, and "RT" for reverse transcriptase with *envZ*-specific cDNA as the template. (C) The expression of *ompR* and *envZ* was quantified by qRT-PCR on strains AB5075 and KT4 (Δ*ompR*). Data are presented as the fold changes in expression ± the standard deviations for three replicates, as calculated by the Pfaffl method. (D) Expression of *ompR* and *envZ* was quantified by qRT-PCR on strain AB5075 grown with or without sodium chloride supplementation. Data are presented as fold changes in expression ± the standard deviations for three replicates, as calculated by the Pfaffl method.

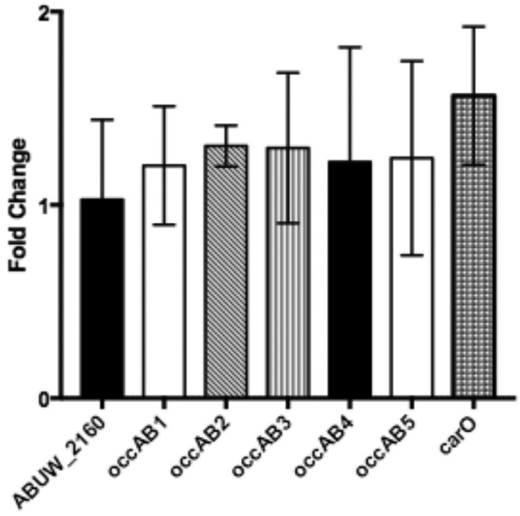

FIG 5 The expression of putative outer membrane proteins is not regulated by OmpR. Quantitative real-time PCR was performed on strains AB5075 and KT4 (Δ*ompR*). The expression of putative outer membrane proteins encoded by ABUW_2160 (the putative *ompC* homolog), *occAB1* to *occAB5*, and *carO* in the Δ*ompR* mutant compared to the wild-type strain AB5075 is shown with target genes listed below the bars. Data are presented as the fold changes in expression ± the standard deviations for three replicates, as calculated by the Pfaffl method.

osmolarity (13). *A. baumannii* encodes a putative homolog (ABUW_2160) of the *E. coli* outer membrane protein OmpC, but the homology is low and the proteins share only 27% identical residues over a portion of the sequence. Homology searches have failed to locate an OmpF homolog gene on the AB5075 genome. Expression of ABUW_2160 was examined in the Δ*ompR* mutant by qRT-PCR, and no change in expression at the transcriptional level was detected (Fig. 5). *A. baumannii* encodes five homologs of the *Pseudomonas aeruginosa* OprD outer membrane protein, named OccAB1 to OccAB5, and four of these have recently been crystallized (31). Zahn et al. found that all of the *occAB* channels had relatively small pore sizes that displayed some specificity and could allow small substrates to traverse the outer membrane, which may correlate with impermeability of the *A. baumannii* outer membrane (31). These genes also represented good candidates for encoding osmotically regulated outer membrane proteins that may be dysregulated in the Δ*ompR* mutant, leading to osmotic sensitivity. The expression of these five genes was quantified by qRT-PCR, and no differences in expression were detected when we compared the Δ*ompR* mutant to the wild-type strain AB5075 under the conditions tested (Fig. 5). An outer membrane protein, CarO, shown to play a role in carbapenem resistance and ornithine uptake was also investigated for differential regulation in the Δ*ompR* mutant (32). CarO expression was unchanged in the Δ*ompR* mutant compared to the wild-type strain AB5075 (Fig. 5). These data suggest that an undiscovered outer membrane protein may be dysregulated when *ompR* is mutated, which leads to sensitivity to sodium chloride in growth medium (Fig. 2).

OmpR and EnvZ are required for virulence in the *Galleria mellonella* infection model. The opaque variant of *A. baumannii* strain AB5075 is more virulent in *G. mellonella* than the translucent variant (10). This led us to investigate the opaque variants of the Δ*ompR*, Δ*envZ*, and Δ*ompR* Δ*envZ* mutants in the *G. mellonella* infection model and assess their virulence compared to the opaque variant of the wild-type strain AB5075. Figure 6A shows that the opaque variant of all three mutants are similarly attenuated (<45% mortality) in *G. mellonella* larvae compared to the wild-type strain AB5075 that exhibits approximately 85% mortality. The wild-type strain AB5075 translucent variant has been shown to be attenuated compared to the opaque variant in the *G. mellonella* infection model (10). Investigation of the translucent variants of the wild-type strain AB5075 and the Δ*ompR* mutant indicated that the mutation does not increase survival of *G. mellonella* larvae (Fig. 6B). These results suggest that the

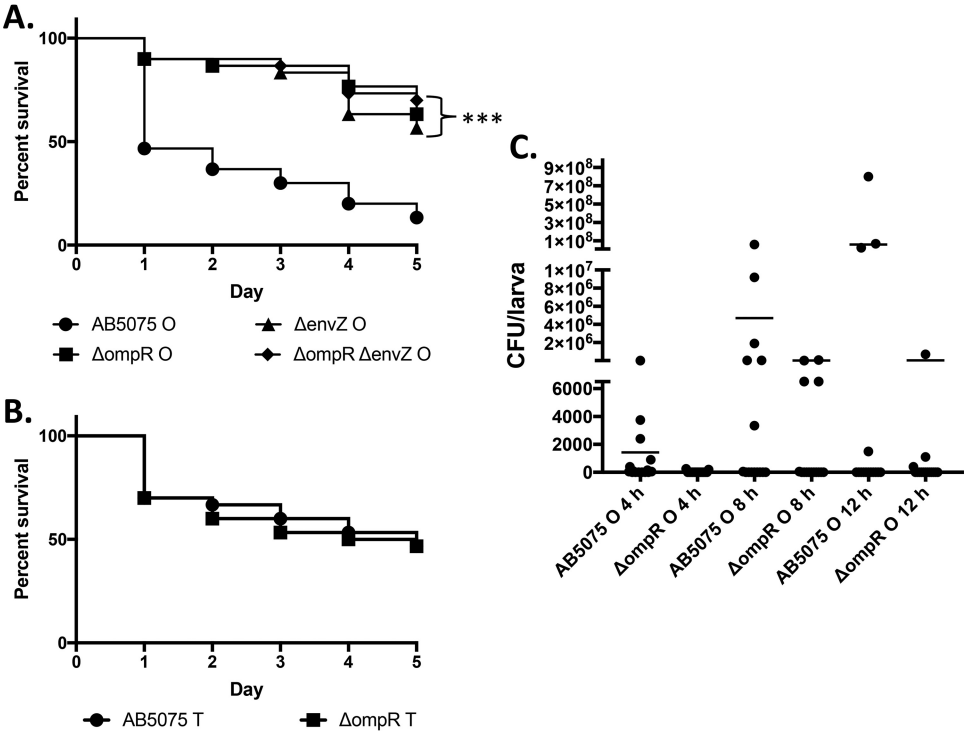

FIG 6 OmpR and EnvZ are required for *A. baumannii* virulence in the *G. mellonella* infection model. (A) *G. mellonella* larvae ($n = 30$) were inoculated with 10^3 to 10^4 CFU of the opaque variant of wild-type strain AB5075 or the isogenic mutants (KT4, KT5, and KT6) as indicated below the graph. Survival was monitored daily for 5 days. ***, $P < 0.0001$. (B) *G. mellonella* larvae ($n = 30$) were inoculated with 10^3 to 10^4 CFU of the translucent variant of wild-type strain AB5075 or the Δ*ompR* mutant (KT4). Survival was monitored for 5 days. (C) *G. mellonella* larvae ($n = 15$) were inoculated as described above with the opaque variant of the wild-type strain AB5075 and the Δ*ompR* mutant. Larvae were sampled at 4, 8, or 12 h postinfection and disrupted to quantify the CFU/larva over time. Each dot represents the CFU count for an individual larva, and lines indicate the average CFU/larva for each strain and time point.

ompR-envZ orthologs are required for the virulence of the opaque variant of *A. baumannii* strain AB5075 in the *G. mellonella* infection model.

Further investigation of *G. mellonella* infection with the opaque variants of the wild-type strain AB5075 and the Δ*ompR* mutant showed that the wild-type strain can establish a more robust infection at 4 h postinfection (Fig. 6C). Larvae infected with the wild-type strain harbored a 2- to 3-log increase in average CFU counts compared to the Δ*ompR* mutant at 4 h (1.4×10^3 versus 3.0×10^1), 8 h (4.7×10^6 versus 8.2×10^3), and 12 h (5.9×10^7 versus 4.8×10^4) postinfection. The postinfection phase variation frequencies were approximately 0.039% ± 0.049% for the wild-type strain AB5075 and approximately 0.32% ± 0.32% for the Δ*ompR* mutant. These frequencies are slightly increased compared to the starting inoculum for both strains but the strong shift to the translucent variant that occurs in colonies of the Δ*ompR* mutant is not present (Fig. 1D).

DISCUSSION

In this study, a null allele in an *ompR* ortholog produced a drastic 401-fold increase in the opaque to translucent colony morphology in *Acinetobacter baumannii* strain AB5075 (Fig. 1). Adjacent to *ompR* is a putative *envZ* ortholog (part of a two-component regulatory system [TCS]), which was also found to repress the opaque-to-translucent-phase variation in *A. baumannii* strain AB5075. In addition, both *ompR* and *envZ* mutations slightly altered the frequency of the translucent-to-opaque switch (Fig. 1E), although these effects were relatively small compared the opaque to translucent. The elevated opaque to translucent switching frequency in the *ompR*, *envZ*, or *ompR-envZ* double mutant could be complemented by providing intact copies of the gene corresponding to each mutation on a plasmid (Table 1). Motility in *A. baumannii*

requires the OmpR/EnvZ TCS, but this system does not play a role in biofilm formation under the conditions tested (Fig. 3; also see Fig. S4 in the supplemental material). This study also demonstrated that *ompR* and *envZ* are part of the same transcript and that OmpR does not exhibit autoregulation under the conditions tested (Fig. 4). Also, null alleles in either *ompR* or *envZ* attenuated the opaque variant of *A. baumannii* strain AB5075 in *G. mellonella*, suggesting that this TCS plays a role in regulating pathogenesis in an invertebrate infection model (Fig. 6A). Assessment of postinfection bacterial load in *G. mellonella* indicated that OmpR is required for *A. baumannii* to establish a robust infection (Fig. 6C).

In *E. coli*, OmpR controls differential regulation of the *ompF* and *ompC* porin genes in response to shifts in osmolarity of the environment to allow for growth at high osmolarity. Phenotypically, OmpR in *A. baumannii* appears to fulfill a role similar to the homologous protein in *E. coli* with regard to the osmotic stress response (14). For example, OmpR is required for *A. baumannii* to grow normally in the presence of sodium chloride as an osmolyte in growth medium (Fig. 2). To date, there is limited information regarding porins in *A. baumannii*, although a few have been investigated and were found to play roles in processes unrelated to osmotic regulation (i.e., nutrient acquisition, antibiotic resistance, oxidative stress, and pathogenesis) (32–34). Based on amino acid homology, we hypothesized that ABUW_2160 encoded an OmpC ortholog. Although our data indicate that ABUW_2160 transcription was not regulated by OmpR, it may still represent an OmpC ortholog that is posttranscriptionally regulated via an OmpR-regulated small RNA (35). A recent study by Zahn et al. indicated that five outer membrane carboxylate channels (OCCs) are encoded on the *A. baumannii* genome, and these channels were shown to have small pores which may contribute to the low permeability of the outer membrane (31). The OCCs were also shown to exhibit some substrate specificity, which may indicate a role for these channels in nutrient acquisition. Mutation of *ompR* did not alter transcription of these channels (Fig. 5), but again this does not rule out OmpR-mediated posttranscriptional regulation of OCC protein expression.

A. baumannii OmpR may act as a global regulator of transcription, as it does in *E. coli*, and RNA sequencing studies are in progress (17). Analysis of the OmpR regulon may indicate potential candidate OMPs and may provide clues to the source of attenuation of virulence in the *ompR envZ* mutants. Mutation of *ompR* does not affect its own expression and other regulatory aspects of *ompR-envZ* transcription in *A. baumannii* are currently unknown. In *E. coli*, *ompR-envZ* transcription is regulated by cyclic AMP, and the catabolite activator protein (known also as CAP or *crp*) (36). *A. baumannii* encodes a CAP homolog known as Vfr (47% identity and 73% similarity to CAP from *E. coli*) that also has strong homology to the same protein in *P. aeruginosa* and has not been shown to play a role in catabolite repression. The Crc protein has been shown to function in catabolite repression in *Acinetobacter baylyi* (a nonpathogenic *A. baumannii* relative), but Crc has not been associated with the osmotic stress response in this organism (37).

Although mutation of *ompR* and/or *envZ* demonstrated similar effects with respect to phase variation frequency in the opaque variant, mutation of *envZ* did not confer sensitivity to osmotic stress. Furthermore, differences in motility between the *envZ* single mutant and the *ompR envZ* double mutant indicate that both components of this regulatory system may affect gene expression exclusive from the other. This suggests that EnvZ may have a differential effect on global transcription compared to OmpR, possibly via signaling through other response regulators. Another possibility is that OmpR maintains partial regulatory function without EnvZ since OmpR has been shown to regulate genes differentially based on its phosphorylation state in *E. coli* (38).

Two-component systems may be attractive targets for the development of anti-infective compounds that alter metabolism or virulence without the strong counter-selection that typically accompanies bactericidal antimicrobials (39). Small molecules that target TCS signal transduction in prokaryotes have been shown to alter virulence factor expression and pathogenesis in enterohemorrhagic *E. coli*, *S. enterica* serovar Typhimurium, and *Francisella tularensis* (40). If phase variation in *A. baumannii* is a

TABLE 2 Strains and plasmids used in this study

Strain or plasmid	Relevant genotype or phenotype[a]	Reference or source
Strains		
E. coli EC100D	F$^-$ *mcrA* Δ(*mrr-hsdRMS-mcrBC*) ϕ80d*lacZ*ΔM15 Δ*lacX74 recA1 endA1 araD139* Δ(*ara-leu*)*7697 galU galK* λ$^-$ *rpsL nupG pir*$^+$ (DHFR)	Epicentre
A. baumannii		
AB5075	Wild type	44
AB-Tn-6A	*ompR*::Tet^r transposon mutant	This study
KT4	Δ*ompR* deletion mutant derived from AB5075	This study
KT5	Δ*envZ* deletion mutant derived from AB5075	This study
KT6	Δ*ompR* Δ*envZ* double mutant derived from AB5075	This study
Plasmids		
pWH1266	*E. coli*/*A. baumannii* shuttle vector	22
pEX18Tc	Suicide vector for *A. baumannii*	41
pompR	*ompR* expressed from pWH1266	This study
penvZ	*envZ* expressed from pWH1266	This study
pompRenvZ	*ompR* and *envZ* expressed from pWH1266	This study
pΔompR	*ompR* deletion in pEX18Tc	This study
pΔenvZ	*envZ* deletion in pEX18Tc	This study
pΔompRΔenvZ	*ompR* and *envZ* deletion in pEX18Tc	This study

[a]Tet^r, tetracycline resistance.

critical virulence factor, then molecules that perturb signal transduction through the OmpR/EnvZ TCS could be utilized as anti-infectives.

MATERIALS AND METHODS

Bacterial strains, plasmids, and growth conditions. The bacterial strains utilized in this study are listed in Table 2. The strains of *A. baumannii* and *E. coli* were maintained at −80°C in 15% glycerol. Bacteria were inoculated into LB broth without sodium chloride cultures to begin each experiment. When required to maintain plasmids, cultures were supplemented with tetracycline at 5 or 10 μg/ml for *A. baumannii* or *E. coli*, respectively.

For growth curves in LB medium with sodium chloride, starter cultures were grown overnight at room temperature prior to inoculation into LB broth containing various concentrations of sodium chloride. Media with various concentrations of sodium chloride (0 to 60 mM) were inoculated with 50 μl of starter culture and grown at 37°C with vigorous shaking. Growth was monitored over time by measuring optical density at 660 nm (OD_{660}).

To generate an expression plasmid for *ompR*, an 884-bp DNA fragment, which began 77 bp upstream from the *ompR* start codon and ended 42 bp downstream from the *ompR* stop codon, was amplified by PCR using chromosomal DNA from *A. baumannii* strain AB5075 as the template (Phusion Hot Start polymerase; Thermo Scientific, Waltham, MA). The fragment was purified from an agarose gel slice and ligated (Fast-Link Ligase; Epicentre, Madison, WI) into pWH1266 (22) that had been digested with ScaI (New England BioLabs, Ipswich, MA) and subsequently treated with shrimp alkaline phosphatase (New England BioLabs) to dephosphorylate linearized vector. The ligation was transformed into *E. coli* Transformax EC100D competent cells (Epicentre) and plated on LB-tetracycline agar (LB+tetracycline) plates, resulting in the expression vector pompR.

To generate an expression plasmid for *envZ*, a 1,514-bp DNA fragment, which began 17 bp upstream from the *envZ* start codon and ended 39 bp downstream from the *envZ* stop codon, was amplified by PCR using *A. baumannii* AB5075 chromosomal DNA as the template. This fragment was cloned into pWH1266 as described for pompR to produce the expression vector penvZ.

To generate an expression plasmid for *ompR-envZ*, a 2,356-bp DNA fragment, which began 77 bp upstream from the *ompR* start codon and ended 39 bp downstream from the *envZ* stop codon, was amplified by PCR using *A. baumannii* AB5075 chromosomal DNA as the template. This fragment was cloned into pWH1266 as described above to produce the expression vector pompR-envZ. The plasmids utilized in this study are listed in Table 2, and the primers are listed in Table 3.

Generation of mutant strains. Mutant *A. baumannii* strains were generated as previously described by Hoang et al. (41). Mutant alleles were generated by PCR amplification of up- and downstream fragments of each gene which were ligated together to produce in-frame deletions for cloning into the pEX18Tc suicide vector (41). Mutant alleles contain deletions corresponding to amino acids 80 to 247 for *ompR* (66% of the protein sequence) and amino acids 211 to 479 for *envZ* (55% of protein the sequence). To delete *ompR* and *envZ* together, the DNA sequence corresponding to amino acid 80 of *ompR* to amino acid 479 of *envZ* (89% of the protein sequences of *ompR* and *envZ*) was removed. Oligonucleotide primers used to generate mutant alleles were engineered to include BamHI restriction sites, and the primers are listed in Table 3. The fragments were digested with BamHI (New England BioLabs) and ligated into pEX18Tc that had been previously digested. These ligations produced the suicide vectors pΔompR,

TABLE 3 Primers used in this study

Primer	Sequence (5′−3′)[a]
ompR expression primers	
ompR Exp. 1.1	TTATACTGAGGGCTTGTTGGC
ompR Exp. 2	GCGGTGGTATTGGCTCTAAA
ompR mutation primers	
ompR Up-1	AAAAAGGATCCCTCGTACGTTTAGGACGGTA
ompR Up-2	TAAACCATCTTCAACGGGCAA
ompR Down-1	TTTGTTCCGGATGGTGCT
ompR Down-2	AAAAAGGATCCGGGGTTTAAACTGAACCACC
envZ expression primers	
envZ Exp. 1.1	GCTTGAGATAAAATAGAGTGAGT
envZ Exp. 2	GAGGTTTAAAATAGCGCTTTAAAT
envZ mutation primers	
envZ Up-1	AAAAAGGATCCAGTATTGCGTCGTCAGGTAC
envZ Up-2	TGGTCGGTTCATTTGTCGAA
envZ Down-1	ACTTTAAGTGAGCGCTTTTAATTT
envZ Down-2	AAAAAGGATCCGCGTTTGCAATTGAACCGAT
ompR-envZ intergenic primers	
R/Z ig 1	TGAACTTGGCTCGTGGCCGT
R/Z ig 2	AACGTTCCCATCGGGTCCGT
Quantitative real-time PCR primers	
clpX qRT For	GCGTTTGAAAGTCGGGCAAT
clpX qRT Rev	CCATTGCAAACGGCACATCT
envZ qRT 1	CCCGCTAGCATGATTCGTCT
envZ qRT 2	TTGCAAAATGCTGCCAACGA
ABUW_2160 qRT 1	TGGGGTAAAAGGCGAAGAGA
ABUW_2160 qRT 2	TAACGTACCGACGCCTTCAG
occAB1 qRT 1	TCGTTGGTTTCGGTGTAGGC
occAB1 qRT 2	AGAAACGTGCCTTAACGCTG
occAB2 qRT 1	GCTTGCAACGGCAGGTTTTA
occAB2 qRT 2	GCGTACCAATGCGTAACTCG
occAB3 qRT 1	TCCCCTATCCGCGCATTTTT
occAB3 qRT 2	TGGGCTACATGCAGTCGTTT
occAB4 qRT 1	TTGCGTTTAAGCCGGGAATG
occAB4 qRT 2	TGGAGAGTCGGCTTACCCAT
occAB5 qRT 1	GGCCAGGCAGTAGTCTTTA
occAB5 qRT 2	TTGGTTTGGGGTACCAGCAG
carO qRT 1	GGCGGATGAAGCTGTTGTTC
carO qRT 2	GTCACCGCCGTTATAACCCA
ompR qRT 1	AAGGTTCACGTGGATGCTGT
ompR qRT 2	CGCCAAGCCAACAAGTTGAA
ompR qRT1.1	GCATCATGGGCAGAAAGCCT
ompR qRT2.1	TGCTGAACATCCTGAAACCG

[a]Underlined sequences denote the restriction sites utilized for cloning.

pΔenvZ, and pΔompRΔenvZ. To transfer the mutant alleles to the chromosome of *A. baumannii* strain AB5075, suicide vector was electroporated into competent AB5075 cells which had been grown overnight in LB medium and washed with 300 mM sucrose, as described by Choi and Schweizer (42). Integrants were selected on LB+tetracycline (5 μg/ml). Counterselection was carried out at room temperature on LB medium without NaCl and supplemented with 10% sucrose. Potential mutants were screened by PCR amplification with the proper primers and confirmed by DNA sequencing.

Phase variation switching frequency determination. For colony switching frequency determination, cultures of each strain were grown to an OD_{600} ~0.5 in LB medium without sodium chloride (supplemented with tetracycline to maintain plasmids when required), and cultures were serially diluted and plated on 0.5× LB medium–0.8% agar (supplemented with tetracycline when required), and dilution plates were grown at 37°C for 24 h. Isolated colonies were picked from plates in triplicate in two separate experiments and resuspended in LB medium with 15% glycerol prior to storage at −80°C. Cell suspensions were thawed, serially diluted in LB medium, and plated on 0.5× LB medium without sodium chloride but with 0.8% agar. The plates were incubated at 37°C overnight, and the CFU per milliliter and the numbers of variant colonies were determined.

Surface motility assays. Cultures of opaque and translucent variants of all strains were grown to mid-log phase (OD_{600} ~0.3) at 37°C in LB medium. A 1-μl aliquot of each strain was spotted in duplicate

onto 0.3% Eiken agar plates, after which plates without sodium chloride were incubated for 9 h and plates with sodium chloride were incubated for 14 h at 37°C. Motility diameters were measured, and the values of four independent measurements for each strain were determined.

Biofilm assays. Opaque and translucent variants of all strains were grown to mid-log phase (OD_{600} ~0.3) in LB medium, and 150-μl aliquots were used to inoculate eight wells of a polystyrene 96-well microtiter plate. The plates were incubated at 37°C for 24 h, and the OD_{600} for each well was determined with a Synergy 4 plate reader (BioTek, Winooski, VT) to determine growth. The medium was decanted and replaced with 250 μl of 10% crystal violet solution, and biofilms were stained for 20 min at room temperature. Each well was then rinsed with distilled H_2O three times and allowed to dry. The crystal violet was solubilized by addition of 300 μl of 33% acetic acid and then diluted 1:10 in 33% acetic acid. The absorbance of each sample was read at 585 nm. Uninoculated LB medium in eight wells per plate served as a negative control that was used to correct the OD_{600} and A_{585} values. The experiments were repeated in triplicate.

RNA isolation. Cultures of the *A. baumannii* strain AB5075 and the Δ*ompR* mutant were grown in LB medium without sodium chloride at 37°C with shaking to an OD_{600} of ~0.7. The cells were harvested from cultures by centrifugation, and RNA was isolated using a MasterPure RNA purification kit according to the manufacturer's protocol (Epicentre). Contaminating DNA was removed by treatment with Turbo DNA-free according to the manufacturer's protocol (Ambion, Waltham, MA). DNA contamination was evaluated by PCR with purified RNA as the template, and the RNA concentration was quantified with a NanoDrop ND-1000 spectrophotometer.

Operon mapping. RNA harvested from the wild-type strain AB5075 was utilized to map the *ompR-envZ* transcript. cDNA synthesis was carried out with the primer envZ Up-2 to yield cDNA specific to the e*nvZ* transcript. To confirm that *ompR* is transcribed with *envZ*, PCR was performed with *envZ*-specific cDNA and primers spanning the predicted intergenic region between *ompR* and *envZ* (R/Z ig 1 and R/Z ig 2).

Quantitative real-time PCR. Total RNA (1 μg) purified from strains AB5075 and Δ*ompR* were converted into cDNA by using the iScript cDNA synthesis kit (Bio-Rad, Hercules, CA) with random primers and SuperScript III reverse transcriptase (Invitrogen, Waltham, MA). The cycling conditions for cDNA synthesis were as follows: 25°C for 5 min, 42°C for 45 min, and 85°C for 5 min. cDNA reactions were then diluted 1:10 with sterile H_2O supplemented with 10 μg of yeast t-RNA (Roche, Indianapolis, IN)/ml. Diluted cDNA was used as the template for experimental reactions. Oligonucleotide primer pairs for quantitative real-time PCR (qRT-PCR) were generated by using the Primer-BLAST program (www.ncbi.nlm.nih.gov/tools/primer-blast/). Primers were designed to amplify ~150-bp fragments for each gene of interest. qRT-PCR was performed using iQ SYBR green Supermix (Bio-Rad) with a Bio-Rad CFX Connect cycler. The following cycling parameters were utilized to amplify and quantify the fragments: 95°C for 3 min, followed by 40 cycles of 95°C for 10 s, 55°C for 10 s, and 72°C for 20 s. Melting-curve data were collected to ensure the proper amplification of target genes. Data were generated from three separate RNA isolations and cDNA preparations and from at least two technical replicates for each primer set. The relative expression of each gene was determined by comparing target gene expression with control gene (*clpX*) expression using the Pfaffl method (43).

***Galleria mellonella* infection model.** *G. mellonella* wax moth larvae were purchased from Wild Bird Goodies, Inc. (Cumming, GA). A 2-ml culture was inoculated with opaque variants of each strain and grown in LB medium without sodium chloride at 37°C to an OD_{600} of ~0.7 (average CFU/ml counts of approximately 8,000, 13,200, 10,746, and 10,720 for the wild-type strain AB5075, the Δ*ompR* mutant, the Δ*envZ* mutant, and the Δ*ompR* Δ*envZ* mutant, respectively). Serial dilutions were prepared in cold LB medium, and cells of each strain were injected into the hemolymph of *G. mellonella* (200 to 250 mg each). Larvae were incubated in petri plates at 37°C in a humidified incubator. At 24-h intervals, viability was assessed by checking for movement; larvae not exhibiting any movement after prodding with a pipette tip were considered dead and were typically dark brown to black. For all experiments, the serial dilutions used for the inoculations were also plated on 0.5× LB medium–0.8% agar plates to determine the overall colony counts. The average phase variation frequencies were determined for all strains to assess the relative number of opaque (virulent) colonies injected based on the starting CFU; the wild-type strain AB5075 (0.0039% average switching frequency) contained an average of 8,000 opaque cells injected, the Δ*ompR* (4.9%) mutant contained approximately 12,600 opaque cells, the Δ*envZ* (3.6%) mutant contained approximately 10,400 opaque cells, and the Δ*ompR* Δ*envZ* (0.0027%) mutant contained approximately 10,700 opaque cells. The reported values represent three independent experiments with at least 10 larvae per strain for each experiment.

For postinfection CFU counts, *G. mellonella* larvae were injected with wild-type strain AB5075 opaque variant at approximately 13,500 CFU per larva (0.0044% average switching frequency) or the Δ*ompR* mutant at approximately 10,730 CFU per larva (0.031% average switching frequency). Larvae were removed from a 37°C incubator at 4, 8, or 12 h postinfection and placed in microcentrifuge tubes containing LB medium plus 15% glycerol. Larvae were disrupted with a pipette tip and vortexed prior to storage at −80°C. The CFU/larva and the switching frequency rates postinfection were determined by plating dilutions from each larva on 0.5× LB medium– 0.8% agar supplemented with ciprofloxacin at 5 μg/ml to reduce the growth of non-*Acinetobacter* organisms.

Statistical analyses. Statistical analyses for phase variation switching frequency determination, surface motility assays, and biofilm assays were conducted with a one-way analysis of variance (ANOVA), followed by Tukey's test for multiple comparisons as included in Prism 7 (GraphPad Software, Inc., La Jolla, CA). Quantitative real-time PCR results were analyzed by one-way ANOVA with Dunnett's post test

using *clpX* as the control in Prism 7. Survival curves were plotted using Prism 7 and assessed for statistical significance by the log-rank test.

SUPPLEMENTAL MATERIAL

Supplemental material for this article may be found at https://doi.org/10.1128/JB.00705-16.

TEXT S1, PDF file, 0.2 MB.

ACKNOWLEDGMENTS

This study was funded by grant 1R21AI115183 from the National Institutes of Health and by funds from the Atlanta Research and Education Foundation. P.N.R. is also supported by grants from the Merit Review program and a Research Career Scientist Award, both from the Department of Veterans Affairs.

REFERENCES

1. Rice L. 2008. Federal funding for the study of antimicrobial resistance in nosocomial pathogens: no ESKAPE. J Infect Dis 197:1079–1081. https://doi.org/10.1086/533452.
2. Potron A, Poirel L, Nordmann P. 2015. Emerging broad-spectrum resistance in *Pseudomonas aeruginosa* and *Acinetobacter baumannii*: mechanisms and epidemiology. Int J Antimicrob Agents 45:568–585. https://doi.org/10.1016/j.ijantimicag.2015.03.001.
3. Centers for Disease Control and Prevention. 2004. *Acinetobacter baumannii* infections among patients at military medical facilities treating injured U.S. service members, 2002-2004. Morb Mortal Wkly Rep 53:1063–1066.
4. Jawad A, Seifert H, Snelling A, Heritage J, Hawkey P. 1998. Survival of *Acinetobacter baumannii* on dry surfaces: comparison of outbreak and sporadic isolates. J Clin Microbiol 36:1938–1941.
5. Roca I, Espinal P, Vila-Farres X, Vila J. 2012. The *Acinetobacter baumannii* oxymoron: commensal hospital dweller turned pan-drug-resistant menace. Front Microbiol 3:148. https://doi.org/10.3389/fmicb.2012.00148.
6. Vincent J-L, Rello J, Marshall J, Silva E, Martin C, Moreno R, Lipman J, Gomersall C, Sakr Y, Reinhart K. 2009. International study of the prevalence and outcomes of infection in intensive care units. JAMA 302:2323–2329. https://doi.org/10.1001/jama.2009.1754.
7. Kroeger L, Hovde L, Mitropoulos I, Schafer J, Rotschafer J. 2007. Colistin methanesulfonate against multidrug-resistant *Acinetobacter baumannii* in an in vitro pharmacodynamic model. Antimicrob Agents Chemother 51:3431–3433. https://doi.org/10.1128/AAC.01433-06.
8. Corvec S, Poirel L, Naas T, Drugeon H, Nordmann P. 2007. Genetics and expression of the carbapenem-hydrolyzing oxacillinase gene bla_{OXA-23} in *Acinetobacter baumannii*. Antimicrob Agents Chemother 51:1530–1533. https://doi.org/10.1128/AAC.01132-06.
9. Lee H-Y, Chen C-L, Wu S-R, Huang C-W, Chiu C-H. 2014. Risk factors and outcome analysis of *Acinetobacter baumannii* complex bacteremia in critical patients. Crit Care Med 42:1081–1088. https://doi.org/10.1097/CCM.0000000000000125.
10. Tipton K, Dimitrova D, Rather P. 2015. Phase-variable control of multiple phenotype in *Acinetobacter baumannii* strain AB5075. J Bacteriol 197:2593–2599. https://doi.org/10.1128/JB.00188-15.
11. Stock A, Robinson V, Goudreau P. 2000. Two-component signal transduction. Annu Rev Biochem 69:183–215. https://doi.org/10.1146/annurev.biochem.69.1.183.
12. Laub M, Goulian M. 2007. Specificity in two-component signal transduction pathways. Annu Rev Genet 41:121–145. https://doi.org/10.1146/annurev.genet.41.042007.170548.
13. Mizuno T, Mizushima S. 1990. Signal transduction and gene regulation through the phosphorylation of two regulatory components: the molecular basis for the osmotic regulation of the porin genes. Mol Microbiol 4:1077–1082. https://doi.org/10.1111/j.1365-2958.1990.tb00681.x.
14. Taylor R, Hall M, Enquist L, Silhavy T. 1981. Identification of OmpR: a positive regulatory protein controlling expression of the major outer membrane matrix porin proteins of *Escherichia coli* K-12. J Bacteriol 147:255–258.
15. Nixon B, Ronson C, Ausubel F. 1986. Two-component regulatory systems responsive to environmental stimuli share strongly conserved domains with the nitrogen assimilation regulatory genes *ntrB* and *ntrC*. Proc Natl Acad Sci U S A 83:7850–7854. https://doi.org/10.1073/pnas.83.20.7850.
16. Igo M, Silhavy T. 1988. EnvZ, a transmembrane environmental sensor of *Escherichia coli* K-12, is phosphorylated in vitro. J Bacteriol 170:5971–5973. https://doi.org/10.1128/jb.170.12.5971-5973.1988.
17. Oshima T, Aiba H, Masuda Y, Kanaya S, Sugiura M, Wanner B, Mori H, Mizuno T. 2002. Transcriptome analysis of all two-component regulatory system mutants of *Escherichia coli* K-12. Mol Microbiol 46:281–291. https://doi.org/10.1046/j.1365-2958.2002.03170.x.
18. Schwan W. 2009. Survival of uropathogenic *Escherichia coli* in the murine urinary tract is dependent on OmpR. Microbiology 155:1832–1839. https://doi.org/10.1099/mic.0.026187-0.
19. Dorman C, Chatfield S, Higgins C, Hayward C, Dougan G. 1989. Characterization of porin and *ompR* mutants of a virulent strain of *Salmonella typhimurium*: *ompR* mutants are attenuated in vivo. Infect Immun 57:2136–2140.
20. Bernardini M, Fontaine A, Sansonetti P. 1990. The two-component regulatory system OmpR-EnvZ controls virulence of *Shigella flexneri*. J Bacteriol 172:6274–6281. https://doi.org/10.1128/jb.172.11.6274-6281.1990.
21. Reboul A, Lemaitre N, Titecat M, Merchez M, Deloison G, Ricard I, Pradel E, Marceau M, Sebbane F. 2014. *Yersinia pestis* requires the two-component regulatory system OmpR-EnvZ to resist innate immunity during the early and late stages of plague. J Infect Dis 210:1367–1375. https://doi.org/10.1093/infdis/jiu274.
22. Hunger M, Schmucker R, Kishan V, Hillen W. 1990. Analysis and nucleotide sequence of an origin of DNA replication in *Acinetobacter calcoaceticus* and its use for *Escherichia coli* shuttle plasmids. Gene 87:45–51. https://doi.org/10.1016/0378-1119(90)90494-C.
23. Shin S, Park C. 1995. Modulation of flagellar expression in *Escherichia coli* by acetyl phosphate and the osmoregulator OmpR. J Bacteriol 177:4696–4702. https://doi.org/10.1128/jb.177.16.4696-4702.1995.
24. Mussi M, Gaddy J, Cabruja M, Arivett B, Viale A, Rasia R, Actis L. 2010. The opportunistic human pathogen *Acinetobacter baumannii* senses and responds to light. J Bacteriol 192:6336–6345. https://doi.org/10.1128/JB.00917-10.
25. Clemmer K, Bonomo R, Rather P. 2011. Genetic analysis of surface motility in *Acinetobacter baumannii*. Microbiology 157:2534–2544. https://doi.org/10.1099/mic.0.049791-0.
26. Eijelkamp B, Stroeher U, Hassan K, Papadimitrious M, Paulsen I, Brown M. 2011. Adherence and motility characteristics of clinical *Acinetobacter baumannii* isolates. FEMS Microbiol Lett 323:44–51. https://doi.org/10.1111/j.1574-6968.2011.02362.x.
27. McQueary C, Kirkup B, Si Y, Barlow M, Actis L, Craft D, Zurawski D. 2012. Extracellular stress and lipopolysaccharide modulate *Acinetobacter baumannii* surface-associated motility. J Microbiol 50:434–443. https://doi.org/10.1007/s12275-012-1555-1.
28. Skiebe E, de Berardinis V, Morczinek P, Kerrinnes T, Faber F, Lepka D, Hammer B, Zimmermann O, Ziesing S, Wichelhaus T, Hunfeld K-P, Borgmann S, Grobner S, Higgins P, Seifert H, Busse H-J, Witte W, Pfeifer Y, Wilharm G. 2012. Surface-associated motility, a common trait of clinical isolates of *Acinetobacter baumannii*, depends on 1,3-diaminopropane. Int J Med Microbiol 302:117–128. https://doi.org/10.1016/j.ijmm.2012.03.003.
29. Vidal O, Longin R, Prigent-Combaret C, Dorel C, Hooreman M, Lejeune P. 1998. Isolation of an *Escherichia coli* K-12 mutant strain able to form

biofilms on inert surfaces: involvement of a new *ompR* allele that increases curli expression. J Bacteriol 180:2442–2449.
30. Pruss B, Besemann C, Denton A, Wolfe A. 2006. A complex transcription network controls the early stages of biofilm development by *Escherichia coli*. J Bacteriol 188:3731–3739. https://doi.org/10.1128/JB.01780-05.
31. Zahn M, Bhamidimarri S, Basle A, Winterhalter M, van den Berg B. 2016. Structural insights into outer membrane permeability of *Acinetobacter baumannii*. Structure 24:221–231. https://doi.org/10.1016/j.str.2015.12.009.
32. Mussi M, Ressing V, Limansky A, Viale A. 2007. CarO, an *Acinetobacter baumannii* outer membrane protein involved in carbapenem resistance, is essential for L-ornithine uptake. FEBS Lett 581:5573–5578. https://doi.org/10.1016/j.febslet.2007.10.063.
33. Rumbo C, Tomas M, Moreira E, Soares N, Carvajal M, Santillana E, Beceiro A, Romero A, Bou G. 2014. The *Acinetobacter baumannii* Omp33-36 porin is a virulence factor that induces apoptosis and modulates autophagy in human cells. Infect Immun 82:4666–4680. https://doi.org/10.1128/IAI.02034-14.
34. Srinivasan V, Vaidyanathan V, Rajamohan G. 2014. AbuO, a TolC-like outer membrane protein of *Acinetobacter baumannii*, is involved in antimicrobial and oxidative stress resistance. Antimicrob Agents Chemother 59:1236–1245. https://doi.org/10.1128/AAC.03626-14.
35. Chen S, Zhang A, Blyn L, Storz G. 2004. MicC, a second small-RNA regulator of Omp protein expression in *Escherichia coli*. J Bacteriol 186:6689–6697. https://doi.org/10.1128/JB.186.20.6689-6697.2004.
36. Scott N, Harwood C. 1980. Studies on the influence of the cyclic AMP system on major outer membrane protein of *Escherichia coli* K-12. FEMS Microbiol Lett 9:95–98. https://doi.org/10.1111/j.1574-6968.1980.tb05614.x.
37. Zimmermann T, Sorg T, Siehler S, Gerischer U. 2009. Role of *Acinetobacter baylyi* Crc in catabolite repression of enzymes for aromatic compound catabolism. J Bacteriol 191:2834–2842. https://doi.org/10.1128/JB.00817-08.
38. Head C, Tardy A, Kenney L. 1998. Relative binding affinities of OmpR and OmpR-phosphate at the *ompF* and *ompC* regulatory sites. J Mol Biol 281:857–870. https://doi.org/10.1006/jmbi.1998.1985.
39. Barrett J, Hoch J. 1998. Two-component signal transduction as a target for microbial anti-infective therapy. Antimicrob Agents Chemother 42:1529–1536.
40. Rasko D, Moreira C, Li D, Reading N, Ritchie J, Waldor M, Williams N, Taussig R, Wei S, Roth M, Hughes D, Huntley J, Fina M, Falck J, Sperandio V. 2008. Targeting QseC signaling and virulence for antibiotic development. Science 321:1078–1080. https://doi.org/10.1126/science.1160354.
41. Hoang T, Karkhoff-Schweizer R, Kutchma A, Schweizer H. 1998. A broad-host-range Flp-*FRT* recombination system for site-specific excision of chromosomally located DNA sequences: application for isolation of unmarked *Pseudomonas aeruginosa* mutants. Gene 212:77–86. https://doi.org/10.1016/S0378-1119(98)00130-9.
42. Choi K, Schweizer H. 2006. mini-Tn7 insertion in bacteria with single *att*Tn7 sites: example *Pseudomonas aeruginosa*. Nat Protoc 1:153–161. https://doi.org/10.1038/nprot.2006.24.
43. Pfaffl M. 2001. A new mathematical model for relative quantification in real-time RT-PCR. Nucleic Acids Res 29:2003–2007. https://doi.org/10.1093/nar/29.10.2003.
44. Jacobs A, Thompson M, Black C, Kessler J, Clark L, McQueary C, Gancz H, Corey B, Moon J, Si Y, Owen M, Hallock J, Kwak Y, Summers A, Li C, Rasko D, Penwell W, Honnold C, Wise M, Waterman P, Lesho E, Stewart R, Actis L, Palys T, Craft D, Zurawski D. 2014. AB5075, a highly virulent isolate of *Acinetobacter baumannii*, as a model strain for the evaluation of pathogenesis and antimicrobial treatments. mBio 5:e01076-14. https://doi.org/10.1128/mBio.01076-14.